Steam condensation analysis in a power plant condenser

ZBIGNIEW DROŻYŃSKI[*]

Institute of Fluid Flow Machinery, Polish Academy of Sciences, Fiszera 14, 80-231 Gdańsk, Poland

Abstract   Proposed is the analysis of steam condensation in the presence of inert gases in a power plant condenser. The presence of inert, noncondensable gases in a condenser is highly undesirable due to its negative effect on the efficiency of the entire cycle. In general, thermodynamics has not provided an explicit criterion for assessing the irreversible heat transfer process. The method presented here enables to evaluate precisely processes occurring in power plant condensers. This real process is of particular interest as it involves a number of thermal layers through which heat transfer is observed. The analysis was performed using a simple, known in the literature and well verified Berman's model of steam condensation in the presence of non-condensable gases. Adapted to the geometry of the condenser, the model enables, for instance, to recognise places where non-condensable gases are concentrated. By describing with sufficient precision thermodynamic processes taking place in the vicinity of the heat transfer area segment, it is possible to determine the distributions of thermodynamic parameters on the boundaries between successive layers. The obtained results allow for the recognition of processes which contribute in varying degrees to irreversible energy degradation during steam condensation in various parts of the examined device.

Keywords: Condensation; Heat transfer; Inert gases; Power plant condenser

Nomenclature

A – heat exchange surgace, m^2
c – concentration of inert gases

---

[*]Corresponding Author. Email: drozd@imp.gda.pl

d	–	diameter, m
h	–	heat transfer coefficient, $\text{W/m}^2\text{K}$
Ja	–	Jacob number
k	–	thermal conductivity W/m K
l	–	coordinate, m
m	–	mass flow rate, kg/s
NCG	–	noncondensible gases
Nu	–	Nusselt number
n	–	number of tubes
Pr	–	Prandtl number
p	–	pressure, Pa
q	–	heat flux, W/m^2
Re	–	Reynolds number
r	–	number of rows
s	–	entropy, J/kg
TBL	–	turbulent boundary layer
TTD	–	terminal temperature difference, $°\text{C}$
t	–	temperature, $°\text{C}$
T	–	temperature, K
u	–	velocity, m/s
Δh	–	specific enthalpy of condensation, J/kg
Δq	–	heat flux, W/m^2
D_v	–	diffusion coefficient

Greek symbols

ν	–	kinematic viscosity, $\text{m}^2\text{/s}$
ρ	–	density, kg/m^3
Π	–	total entropy increase, W/K
π	–	local entropy increase, $\text{W/m}^2\text{K}$

Subscripts

0	–	steam space area between tubes
a	–	average
c	–	condensate
g	–	gas
i	–	inner
m	–	mixture
o	–	outer
s	–	saturation
t	–	turbulent
v	–	vapour
w	–	cooling water
ci	–	phase boundary
wi	–	inner wall diameter
wo	–	outer wall diameter

1   Introduction

Surface heat exchangers are the most often used elements of the steam Clausius -Rankine cycle. One of the largest heat exchangers in such installations are steam condensers [1–3]. The effectiveness of those devices affects the overall output efficiency of the entire installation. Thermodynamics does not provide an explicit criterion to assess the efficiency of heat transfer phenomena. There is no measure by which one could assess the irreversibility of phenomena based on the second law of thermodynamics. In the power industry for instance, the efficiency of condensers is assessed according to the terminal temperature difference (TTD) between fluids. This parameter allows for assessment of the process at the macro level but not for detailed analysis of the operation of the device as a whole. The discussed method provides a more precise evaluation of local irreversibilities contributing to the final process [4]. Such a precise analysis requires information about local distributions of thermodynamic parameters in particular thermal boundary layers of fluids taking part in heat transfer and temperature distribution in the solid wall between them. In the considered process, a vapour-air mixture is exposed to the cold surface of a heat exchanger with a temperature lower than the saturation temperature [5–11].

Before explaining the full analysis, it is useful to briefly describe the Berman model [12]. This model makes possible calculations of steam condensation mixed with air as a non-condensing gases (NCGs) which resists heat transfer. The presented method is known for a number of simplifications named below. Published model, was later analysed, extended, complemented in numerous publications, and used in calculations [12–19]. In this paper it is extended and adapted to the complex geometry of the condenser. The obtained calculation results describe the complex process of steam condensation in a real device in a way which is very precise and compatible with experimental results. Presented below are the basic assumptions of the Berman model. From it mathematical equations are derived which describe processes taking place in the steam condenser. The most representative calculation results based on those equations are presented. The above approach was used to analyse in detail the condensation process as a phenomenon of heat convection on both sides of the surface and its conduction through the fouled wall [5,6,11,20]. One of the analysed issues was the presence of air as the inertial gas in thermal sublayers (gas blanket) and the effects of its concentration in selected heat transfer areas inside the condenser. The consequences of a liquid film wetting the heat

transfer surface on the condensation process was also analysed. The effect of heat conduction through a diaphragm wall fouled on both sides on the course and results of the entire heat transfer process was assessed at various points in the condenser. The presented calculations make it possible to detect NCGs stagnation areas and, consequently, to indicate places from which air is to be sucked. Results of the calculations can be of considerable value in the designing and operation of power plant steam condensers. The resulting conclusions provide opportunities for further analysis of various factors affecting steam condensation in the condenser. Sample analyses refer to the irreversibility of the heat transfer process. These are based on data collected for a two passes steam condenser, which is the most popular and most accurately examined condenser in Poland.

2 Heat transfer surface and thermal load of the examined object

The presented analysis is based on research performed by the author on a condenser connected to a two-outlet turbine working in a steam cycle with the nominal electric power of 215 MW [4]. Each turbine outlet cooperates with one out of two identical condenser parts, connected with each other on the steam side. In steam cycle condensers, the flows of three fluids can be named: the organised flows of cooling water, steam sucked in by the condenser, and air flow. In terms of the arrangement of the cooling water flow, the heat transfer surfaces in the steam condenser are divided into two passes (pass 1 and pass 2), Fig. 1. In total, the two parts of the device include four second pass condensation bundles, four first pass condensation bundles and four air concentration (air cooler) bundles. Due to their general shape, the condensation bundles are frequently referred to as 'bands'. Each bundle consists of tubes arranged in rows. The rows of tubes in the bundles (bank of tubes) were numbered in the steam flow direction.

The first coolant pass of the condenser (pass 1) consists of four condensation tube bundles (bands) and four air concentration banks. It was assumed that the heat transfer processes in each of the four first pass condensation bundles take exactly the same course. Each band comprises rows $r = 9$ of tubes, with tubes $n = 143$ in each row. In this area heat transfer has the form of a forced convection; therefore these banks are also referred to as condensation bundles. Each band comprising the first pass is directly followed by an air concentration (air cooler) bundle. As in the previous
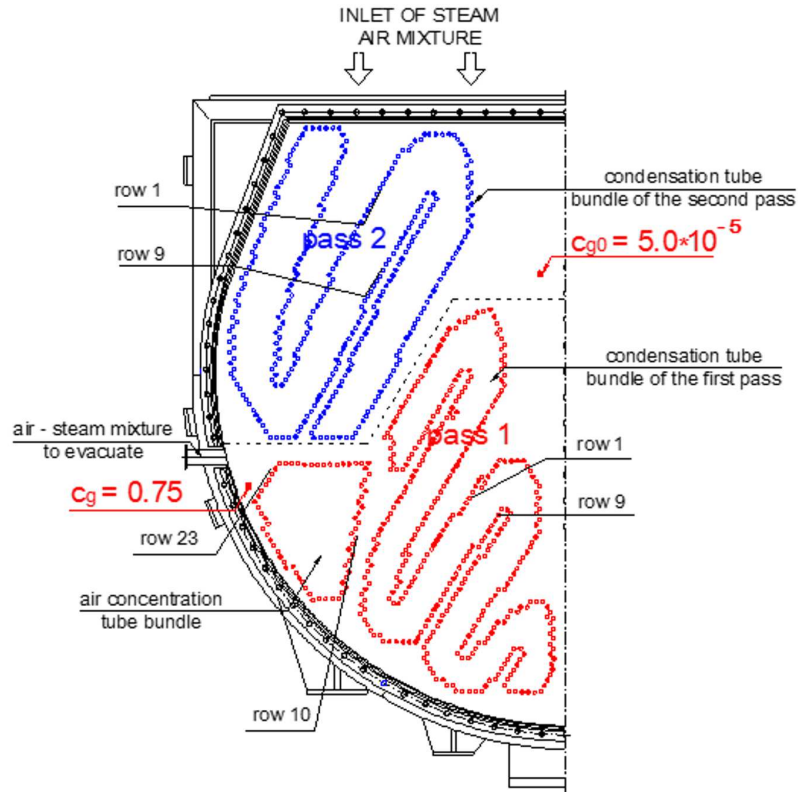
Figure 1: Tube bundles layout in the middle section of one condenser casing with connector pipe of vacuum pump as an air suction point.

case, it was assumed that the heat flow processes in each of the four air concentration bundles take exactly the same course. The first ten rows of this bundle comprise the same number of $n = 28$ tubes. In the next rows the number of tubes decreases to reach $n = 18$ tubes in the last row, $r = 23$. In the last rows of this bundle (the tube nest of the air cooler) heat transfer has the form of free convection. In total, 6612 tubes are installed in the first pass.

The second pass of the condenser (pass 2) comprises four bands. As in the first pass case, it was assumed that the condensation processes in all four tube bundles take exactly the same course. Each bundle consists of $r = 9$ rows of tubes, with $n = 137$ tubes in each row. In this area heat

transfer has, generally, the form of forced convection.

During the measurements, the cooling water mass flow rate was equal to $m_{wt} = 8000$ kg/s. The cooling water temperature at the condenser inlet was $t_{win} = t_{w0} = 19.0$ °C, and after mixing in the return chamber, it increased to $t_{wrev} = 24.7$ °C, to reach $t_{wout} = 28.2$ °C at the condenser outlet. In the first pass, the mass flow rate of the cooling water in a single tube was $m_w = 1.21$ kg/s, and the inlet temperature of the cooling water was $t_{w0}(1 \le r \le 23, l = 0) = 19.0$ °C which corresponds to the Reynolds number $\mathrm{Re}_{w\,pass1} > 5.4 \times 10^4$. In the second pass, the cooling water mass flow rate in a single tube was $m_w = 1.62$ kg/s, and the inlet water temperature was the final effect of cooling water mixing in the condenser return chamber, which corresponded to the Reynolds number $\mathrm{Re}_{w\,pass\,2} > 7.2 \times 10^4$.

The mass flow rate of the steam sucked in by the condenser was equal to $m_v = 127.66$ kg/s, and the pressure in the steam space was $p_0 = 6530$ Pa. Based on the experiments [1,2,20], an assumption was made that the heat exchange on the tubes composing one row in the bundle was the same and changed linearly with the increasing row number in the bundle. Simple measurements performed on the examined condenser and complemented by relevant balance calculations enabled to assess the range of heat exchange as equal to 167.4 MW in tubes comprising the first pass condensation bundle (first pass bands), to 25.0 MW in the air concentration bundles, and to 115.5 MW in the second pass condensation bundles (second pass bands). The mass flow rate of the steam in front of the bundles was assumed constant and equal to $m_v = 79.79$ kg/s for the first pass, and $m_v = 47.87$ kg/s for the second pass.

The above mentioned tubes were typical straight brass tubes of outer/inner diameters of $d_o/d_i = 0.030/0.028$, mounted in a staggered arrangement with the minimal distance of 0.015 m between the surfaces. A total number of 11544 tubes was installed in the examined device, each tube of $L = 9$ m in length. The total heat exchange area was $A_t = 9792$ m^2.

The performed measurements ($t_{win} = t_{w0} = 19.0$ °C and $t_{wout} = 28.2$ °C and the adopted assumptions [1,2,20] made it possible to calculate the heating range of the cooling water in the tubes of successive rows in the condenser bundles, Fig. 2.

Experimental studies have revealed that the concentration of NCGs in the flow entering a condenser cannot be measured in practice [1,2,22]. The basic component of NCGs is air. Mass flow rate measurements of this gas in the condenser were performed using orifice plates installed at outlets

from steam ejectors [10,22]. These measurements made it possible to assess NCGs concentration defined as an air mass fraction $c_g = m_g/(m_g + m_v)$. In a properly working, airtight condenser (Fig. 1) inlet air mass fraction should not exceed $c_{g0} = 5.0 \times 10^{-5}$ [1,2,10,22]. Apart from the already existing leaks, the examined device was additionally aerated via two nozzles: one in each condenser casing. In the analysed case the mass flow rate of the air flow was equal to $m_g = 0.94$ kg/s. As a result, the air concentration in the condenser (air mass fraction) was extremely high, $c_{g0} = 1.1 \times 10^{-4}$, which is much more than the values observed in normal conditions [21,23].
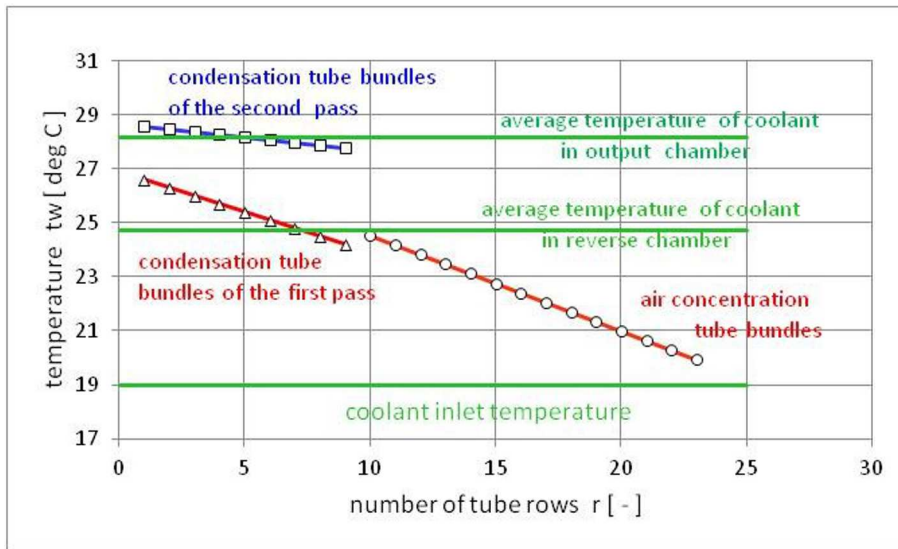

Figure 2: Cooling water temperature in condenser water chambers and at outlets of successive bundle row tubes.

On the other hand, measurements performed in the manifolds used to evacuate harmful gases from condensers [10,22] have shown that NCG concentration can reach approximately $c_g = 0.75$ [1,2,22,23]. When comparing inlet and outlet air mass fractions, we can see that some processes take place in the condenser steam-gas areas which lead to very intensive and unidirectional changes of air concentration. Two active noncondesible gases (NCGs) concentration mechanisms in thermal layers over the heat transfer surface are assumed. One of them, Fig. 3, is drift of the molecules of the NCGs to follow the component of the mixture velocity u_{vp}, which is perpendicular to

the heat transfer surface in the condenser. The other mechanism involves molecules being squeezed out of these gases in the direction of the partial steam pressure gradient, towards also lower values of vapour pressure.

Preliminary calculation results are reported in [4]. According to those data, the terminal temperature difference reached as much as 9.0 K (while the acceptable difference is 2–3 K. At the same time the entropy increase reached 35.91 kW/K for condenser pass 1, and 15.55 kW/K for condenser pass 2. The total entropy increase for the entire device was equal to 51.46 kW/K.

3 Phenomenological model of steam condensation on heat transfer surface

Presented below is a 3D model analysis of heat transfer in a condenser. It assumes that steam flows in a direction perpendicular to the longer sides of the stretched bands. Each of rectangular bank consists of r rows with n tubes in each row. The analysed phenomena are steady and time-independent. Figure 3 shows schematically a fragment of the heat transfer surface cross section with a mixture of two-phase vapour with NCGs on one side, and the cooling water flowing on the other side. Here, the following areas can be named [13,23]:

- steam flow area between the tubes, with parameters p_0, $t_0 \approx t_s\ (p_0)$, in which the mixture flow velocity is $u_v(r)$;
- thermal layer on the condenser steam side with two sublayers:
  - steam-gas sublayer, comprising a mixture of saturated steam, water and NCGs, where the condensation takes place,
  - condensate film which moistens the heat transfer surface,
- diaphragm wall, of known thickness with layers of scales on both sides;
- thermal layer on the cooling water side;
- flow of the heated water with parameters $p_w(r,l)$, $t_w(r,l)$, and u_w;

where r is the number of tube rows in the bundle, and l is the tube length coordinate in the flow direction.

The continuity of temperature distributions in an arbitrary cross-section was assumed for the condensers steam area, diaphragm, and cooling water area. The remaining parameters describing the thermodynamic states of

the fluids (as manifolds) are defined on the open areas of the channels through which the fluids flow. The static pressure on the condenser steam side is constant and equal to p_0 [1,2]. The temperature distribution in the gas layer surrounding the tube induces partial pressure distributions of the steam and air in the mixture.
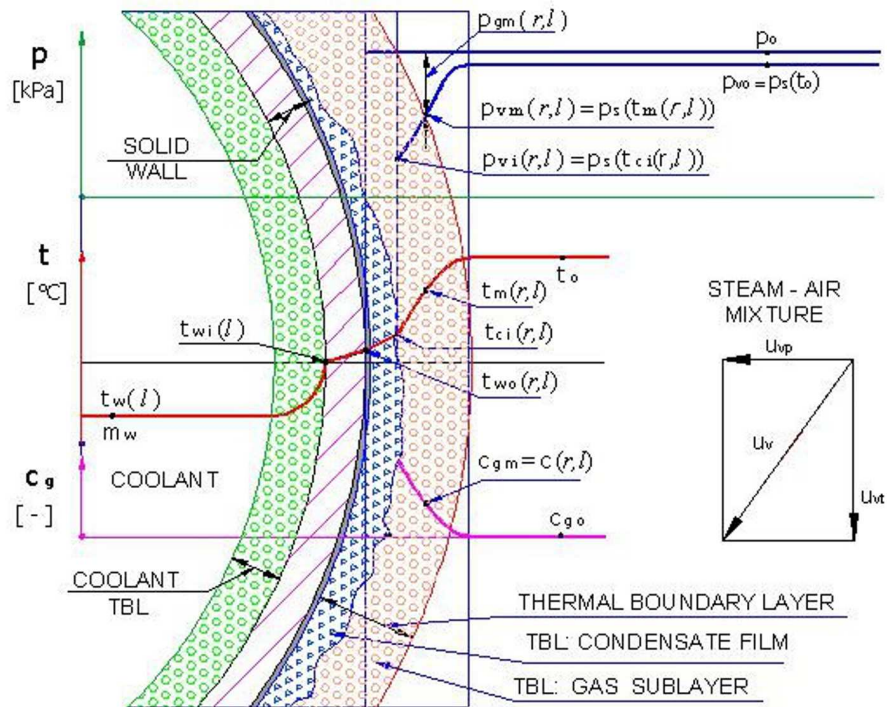

Figure 3: Diagram of the phenomenological model with marked thermal boundary layers on both sides of the tube heat exchange surface in the rth bundle row, with distance l from the cooling water inlet to the tube.

The partial steam pressure in the mixture at a given place in an area of the condenser steam side was assumed to be equal to the saturation pressure for the temperature at this point. According to Dalton's law, the total pressure of the mixture is equal to the sum of the partial pressures of the mixture's components. The heat of NCGs cooling from temperature t_0 in the binary mixture to temperature $t_{ci}(r,l)$ is negligible compared to the latent heat of steam condensation. Furthermore, it has also been assumed that heat of the condensate cooling from temperature t_0 to temperature

$t_{wo}(r,l)$ on the heat transfer surface is small compared to the latent heat released by steam condensation. The Jakob number calculated for the 'supercooled' condensate is low.

4 Mathematical description of the phenomenological model

According to the first law of thermodynamics, basic equations for the given coordinate l in the rth row of the bundle of the given condenser pass take the form [13,23]

$$
\begin{aligned}
\Delta q\,(r,l) =\ & \Delta h\,(r,l)\ \ \beta_v\,(r,l)\ \ \Delta p_v\,(r,l) \\
=\ & h_{cc}\,(r,l)\,[\,t_{ci}\,(r,l) -\ t_{wo}\,(r,l)\,] = k_{wi-wo}[\,t_{wo}\,(r,l) -\ t_{wi}\,(r,l)\,] \\
=\ & h_{cw}\,(r,l)\,[\,t_{wi}\,(r,l) -\ t_w\,(r,l)\,]\,,
\end{aligned}
\tag{1}
$$

where $\Delta p_v(r,l) = p_0 - p_s(t_{ci}(r,l))$ is the partial steam pressure difference in the cross section of the steam-gas sublayer, and $\beta_v(r,l)$ is the mass diffusion coefficient related to the partial steam pressure difference. The heat flux released during steam condensation in the thermal sublayer with the NCGs, next penetrates the condensate film and is conducted by the fouled wall, to finally penetrate the cooling water layer on the other side of the diaphragm. At the present stage of analysis the resultant, overall heat transfer coefficient is calculated as for a flat plate geometry. This simplification, characteristic for the Berman model, avoids the need to determine the condensate film thickness on the horizontal, flooded, vibrating tube, which is always required in cylindrical geometry calculations.

4.1 Process of heat flow through vapour-gas sublayer

When analysing heat transfer through the vapour-gas sublayer, the following assumptions were adopted:

- analysed heat transfer takes place in the direction perpendicular to heat transfer surface;
- saturated steam is treated as a real gas;
- inertial gas, air, is treated as a perfect gas;
- for a given coordinate l in this sublayer, the thermal properties of the mixture are constant and determined for the sublayer's average temperature;

- heat of cooling NCGs is small compared to the latent heat of steam.

The heat transfer analysis in the steam-gas volume of the thermal sublayer made use of results obtained by Berman during experiments [15] to determine heat flux transferred from a steam-gas mixture into a condensate film. The steady inflow of the steam-air mixture leads to the increase of NCGs concentration over the heat transfer surface in the analysed sublayer.

Condensing vapour has to diffuse through the NCGs stagnation area (gas blanket) [24]. For different values of criterial numbers, two heat flow patterns were identified: forced convection for $\text{Re}_v(r) \geq 350$ and free convection for $\text{Re}_v(r) < 350$. The characteristic Nusselt number in the analysed model takes a form

$$\text{Nu}(r,l) = \beta_v\,(r,l)\,\frac{d_o}{D_v\,(r,l)} = \ A\text{Re}_v(r)^{0.5}\left[\frac{\Delta p_v\,(r,l)}{p_0}\right]^{-\frac{1}{3}}\varepsilon_g(r,l)^{-B}\;, \quad (2)$$

where $A = 0.82$, $B = 0.6$ for $\text{Re}_v(r) \geq 350$, and $A = 0.52$, $B = 0.7$ for $\text{Re}_v(r) < 350$. $D_v(r,l)$ is the diffusion coefficient related to thermodynamic parameters of the steam flowing onto the heat transfer surface [6]:

$$D_v\,(r,l) = \ 6.27 \times 10^{-6}\left[\ \frac{T_m(r,l)}{273.15}\ \right]^{0.8}\frac{1}{p_0}\;, \quad (3)$$

$$\varepsilon_g\ (r,l) = \ \frac{p_{gm}(r,l)}{p_0}\;, \quad (4)$$

$$\text{Re}_v\,(r) = \frac{u_{vt}\,(r)\,d_o}{\nu_0}\;. \quad (5)$$

Finally, the heat flux penetrating through the steam-gas volume is determined by the following relations:

$$\Delta q\,(r,l) = A\frac{\triangle h\,(r,l)}{\varepsilon_g\,(r,l)^B d_o}\left[\frac{T_m\,(r,l)}{273.15}\right]^{0.8}\left[\frac{\Delta p_v\,(r,l)}{p_0}\right]^{\frac{2}{3}}\text{Re}_v(r)^{0.5}\;, \quad (6)$$

where $A = 0.520$, $B = 0.6$ for $\text{Re}_v(r) \geq 350$, and $A = 0.330$, $B = 0.7$ for $\text{Re}_v(r) < 350$.

These equations describe heat transfer through the steam-gas part of the thermal layer. Berman's model was successfully used in numerous analyses [1,4–6].

4.2 Process of heat transfer through condensate film

Heat transfer through a film of liquid was analysed by Nusselt (model described in [25–27]) who adopted the following assumptions:

- dominating forces in the condensate layer are viscosity and gravity, while inertia forces can be neglected;

- friction in the phase boundary can be neglected;

- effect of surface tension on the condensate flow can be neglected;

- for the given coordinate *l*, the properties of the condensate film are constant and defined for the average temperature in the film;

- temperature distribution in the layer perpendicular to the tube surface is linear;

- heat which corresponds to the cooling of the condensed liquid from temperature t_0 in the condenser to temperature $t_{wo}(r, l)$ on the heat transfer surface is small compared to the latent heat released by steam condensation [28,29]. The Jakob number calculated for the 'super-cooled' condensate is low.

Taking into account the above assumptions, the following formula describes the temperature drop across the condensate film:

$$t_{ci}\,(r,l) - \ t_{wo}\,(r,l) = \frac{\triangle q\,(r,l)^{\frac{8}{7}}\Big[1 + \frac{m_{gm}(r,l)}{m_{vm}(r,l)}\Big]^{0.0915}}{Z\,(r,l)\ \ [u_v\,(r,l)\,\rho_v\,(r,l)]^{0.183}}\ ,\qquad(7)$$

where

$$Z\,(r,l) = 17400\ k_c\,(t_{ca})\ \rho_c\,(t_{ca})^{0.194}\Big[\frac{\Delta h}{\eta_c\,(t_{ca})}\Big]^{0.143}\rho_v[t_m\,(r,l)]^{-0.0915}\ ,\quad(8)$$

$t_{ca} = t_{ca}(r,l)$ is the average temperature in the film. Nusselt's model has been positively verified in many cases and now is commonly used in analysing heat transfer through layers of liquid.

4.3 Thermal conduction through a fouled wall

The conduction of the heat transfer through a fouled wall is described by the Fourier model. Fouling deposits are usually poor thermal conductors, the prediction on which is based largely on experience. The heat transfer is

modelled parametrically, assuming that the resistance of the heat transfer through the fouling deposit formations are given by a multiple of the resistance of the heat flow through the clean wall. The resistance of the heat transfer through the fouled wall is expressed as

$$\frac{1}{k_{wi-wo}} = \frac{\delta}{k} + R_{fi} + R_{fo} \,, \tag{9}$$

where δ is the channel wall thickness, k is the thermal conductivity of the brass and R_{fi} and R_{fo} are resistances of heat flow through the inner and outer layers of scales, respectively [4,5,21]. In the calculations it was assumed that the resistance of the heat transfer through the fouling deposit layers is equal to that of the heat flow through the clean wall. In a properly working condenser resistance of the heat transfer through the fouling deposits should not exceed resistance of the heat flow through the clean wall.

4.4 Process of heat flow through thermal layer of cooling water

The process was assumed to be fully developed both hydrodynamically and thermally. For the conditions corresponding to $\mathrm{Re}_w > 5.0 \times 10^4$, $0.7 < \mathrm{Pr} < 160$, the phenomenon of heat convection from the tube wall through the boundary layer into the cooling water flow is described by the well-known and verified relation

$$\mathrm{Nu} = 0.023 \, \mathrm{Re}_w^{\frac{4}{5}} \, \mathrm{Pr}^{\frac{1}{3}} \,, \tag{10}$$

where the Prandtl number is calculated for the cooling water pressures ranging between $0.1\,\mathrm{MPa} < p_w(l) < 0.5\,\mathrm{MPa}$ and the temperatures ranging between $0 < t_w(r,l) < 200\,^{\circ}\mathrm{C}$.

The heat transferred over the surface of tube segment dA with dl length heats the liquid flow m_w by $\Delta t_w(r,l)$

$$\Delta q\,(r,l) = m_w c_w \Delta t_w\,(r,l) \,, \tag{11}$$

where c_w is the specific heat of water. This latter equation describes temperature changes of the cooling water along the tube length.

The classic issue of convectional heat transfer across two thermal boundary layers and heat conduction in the wall is described by four (Berman, Nusselt, Fourier and Dittus-Boelter) equations. Mathematically the problem can be presented with a set of equations that enable calculations of:

temperature of the steam-gas mixture – $t_m(r,l)$, temperature on the condensate film interface – $t_{ci}(r,l)$, temperature on the outside – $t_{wo}(r,l)$, and inside – $t_{wi}(r,l)$ of the wall. The described issue concerning steam condensation in multiphase flow with presents of NCGs, as a nonlinear one, requires very precise definition of its domain. Just by precisely describing the mathematical problems of thermodynamics one can ensure the convergence, existence and uniqueness of the solution.

When applied to the condenser's complex geometry, the Berman method makes it possible to determine the thermodynamic parameters of the fluids involved in the heat exchange processes. These parameters can be used to analyse the efficiency of the irreversible heat transfer processes. The problem of the existence and uniqueness of the solution to the nonlinear system of equations was analysed at the research stage described in [23]. The Berman method, which generally makes use of a system of simplifying assumptions, may be extended when necessary. Its basic drawback is the adoption of plane flat geometry. However, this approach allows for the well-known Nusselt solution to be applied. This model should be considered the first approximation of the problem of heat transfer through successive sub-layers, including the film of liquid on a vibrating, condensate-flooded, horizontal tube. The thermodynamic parameters of the fluid on the boundaries of thermal layers, which are needed for calculations, can also be obtained from measurements.

5 Entropy increase as the measure of irreversible energy degradation

The results obtained using the above presented model have the form of thermodynamic parameters of all fluids involved in steam condensation. The calculated parameters enable now to determine local changes of (specific) entropies of these fluids.

By definition [30–32], the local entropy change of the steam condensing on the heat transfer surface $dA(r,l)$ is

$$ds_{T_o}(r,l) = \frac{-\,dq(r,l) + \,dq_{vt}(r,l)}{T_o} \,, \tag{12}$$

where: $dq(r,l)$ – local heat transfer (per unit area) of the steam condensing and $dq_{vt}(r,l)$ – local heat generated (per unit area) in the process of turbulent steam flow both in the condenser steam space. T_o – temperature

of inflowing vapour. By definition, this value of the local entropy change of the higher-temperature medium in the process of heat transfer between potentials is negative. Likewise, for the local entropy change of the cooling water flowing on the other side of the heat transfer surface we have

$$ds_{T_w}(r,l) = \frac{dq(r,l) + dq_{wt}(r,l)}{T_w(r,l)} \ , \tag{13}$$

where $dq(r,l)$ is the local heat transfer (per unit area) which heats the water, and $dq_{wt}(r,l)$ – local heat generated (per unit area) in the process of turbulent flow of cooling water through the tube. T_w is the temperature of cooling water fluids. By definition, this value of the local entropy change of the lower-temperature fluid in the process of heat transfer between potentials is positive. The above formulas determine local entropy changes of the fluids involved in the condensation process in relation to the elementary heat transfer surface $dA(r,l)$.

As mentioned above, in heat and mass transfer process, the change of local entropy of the heating fluid is negative while that of the heated fluid is positive. The sum of local entropy changes of the media involved in this irreversible process (entropy generation) is always positive.

The essence of operation of heat exchangers is that [29,33,34] heat transferred between the media are much larger than the heat generated in the process of turbulent flow of these fluids in channels, i.e., $dq(r,l) \gg dq_{vt}(r,l)$ and $dq(r,l) \gg dq_{wt}(r,l)$. That is why the further part of the analysis will take into account entropy changes only for the irreversible process of heat transfer $dq(r,l)$.

The sum of the entropy changes solely corresponding to the heat transfer [30,35–39] is

$$d\pi_{T_o,T_w}(r,l) = dq(r,l)\left[\frac{1}{T_w(r,l)} - \frac{1}{T_o}\right] =$$
$$\frac{dq(r,l)}{T_w(r,l)}\left[1 - \frac{T_w(r,l)}{T_0}\right] = \frac{dq(r,l)}{T_0}\left[\frac{T_0}{T_w(r,l)} - 1\right] \geq 0 \ , \tag{14}$$

where $d\pi_{To,Tw}(r,l)$ is the local entropy increase (per unit area) in the heat transfer, $dq(r,l)/T_w(r,l)$ is the local value of the entropy change (per unit area) of the heated medium, $dq(r,l)/T_0$ is the local absolute value of the entropy change (per unit area) of the heating medium, $[1 - T_w(r,l)/T_0]$ and $[T_0/T_w(r,l) - 1]$ are the thermodynamic potential coefficient t_s for the entropy change of the lower-temperature (heated) medium and the higher-temperature (heating) medium, respectively. Defined and discussed in [4]

thermodynamic potential coefficient can be consider as a probability of equilibrium state in heat transfer.

The local entropy increase $d\pi_{To,Tw}$ in the heat flow process is equal to zero when $T_w(r,l) = T_0$. For $T_w(r,l) < T_0$ the local entropy increase $d\pi_{To,Tw}$ caused by the heat transfer is always greater than zero (i.e., the heat flow is from T_0 to T_w). The local entropy increase defined in the above way can be interpreted as the measure of irreversible degradation of thermal energy [4] in the heat transfer processes. The essence of this irreversible degradation is that an arbitrary engine fed with degraded (lower-temperature) heat flux will work with lower efficiency.

Having known the entropy changes of one medium taking part in the heat transfer process, (the steam in the heat exchanger, for instance) and the temperature distributions on both sides of the analysed surface fragment, we can calculate the entropy changes for the other medium (for instance, the exhaust gas in the boiler chamber), which can make a piece of valuable reference information.

After adding and simultaneously subtracting the inverse of temperature on subsequent thermal boundaries we arrive at the entropy increase equation in the form

$$
\begin{aligned}
d\pi_{T_o,T_w}\left(r,l\right) &= dq\left(r,l\right)\left[\frac{1}{T_w\left(r,l\right)} - \frac{1}{T_o}\right] \\
&= \frac{dq\left(r,l\right)}{T_{ci}\left(r,l\right)}\left[1 - \frac{T_{ci}\left(r,l\right)}{T_0}\right] + \frac{dq\left(r,l\right)}{T_{wo}\left(r,l\right)}\left[1 - \frac{T_{wo}\left(r,l\right)}{T_{ci}\left(r,l\right)}\right] \\
&\quad + \frac{dq\left(r,l\right)}{T_{wi}\left(r,l\right)}\left[1 - \frac{T_{wi}\left(r,l\right)}{T_{wo}\left(r,l\right)}\right] + \frac{dq\left(r,l\right)}{T_w\left(r,l\right)}\left[1 - \frac{T_w\left(r,l\right)}{T_{wi}\left(r,l\right)}\right] \\
&= d\pi_{T_0,T_{ci}}\left(r,l\right) + d\pi_{T_{ci},T_{wo}}\left(r,l\right) + d\pi_{T_{wo},T_{wi}}\left(r,l\right) + d\pi_{T_{wi},T_w}\left(r,l\right)
\end{aligned}
\tag{15}
$$

in which consecutive terms represent local entropy increases (per unit area) caused by heat transfer through relevant layers and in the exchanger diaphragm. Temperature distributions in successive thermal layers of the media can be obtained from thermal analysis or experimental measurements.

The local entropy increase in the heat transfer between flows of fluids separated by a given heat transfer surface, $dA(r,l)$, is equal to the sum of local entropy increases across the layers of these media and the local entropy increase in the exchanger diaphragm, wall.

The entropy increase caused by the heat transfer between the media through the heat exchange surface, $A(r,l)$, is

$$\Pi_{T_o,T_w} = \int_0^A d\pi_{T_o,T_w}(r,l)dA \,, \tag{16}$$

where $A(r,l)$ is the surface of heat transfer between the media for given r and l.

6   Calculation results

It was assumed that the presence of NCGs is characterised by the air concentration (air mass fraction) in steam-gas sublayer along the tubes of successive rows in the banks, $c_g(r,l)$. The phenomenological model suggests that the inertial gases in the thermal layers should be pushed out towards the lower temperature of the cooling water. Attempts to calculate the non-uniform distribution of NCG concentrations along a tube were performed in [23]. Nevertheless, at this stage of analysis an assumption was made that the distribution of NCGs concentrations along the tubes is constant, which is in line with the assumption that the heat does not flow in this direction [13]. This assumption is also compatible with the structure of the condenser. Inner partitions, baffles, used to hold tubes in the steam space counteract the pushing out of the inertial gases towards the cooling water temperature gradient. That is why further calculations are based on the simplest variant with uniform concentrations of inert gases along the tubes of successive rows in the banks, i.e., $c_g(r,l) = c_g(r)$.

The calculated results have the form of the thermodynamic parameters of the fluids involved in the process of steam condensation in the steam-gas mixture. These parameters are calculated for successive condenser passes, bundles of tubes in the passes, rows r of tubes in the banks, and finally along a single tube, l, in a row. Heat transfer (1) is balanced on 1 m long pipe section just between successive baffles. In sections transverse to the heat transfer surface, the calculated parameters refer to the thermal boundaries. The solutions to the nonlinear set of equations [23] are the distributions of:

- temperature of the fluid involved in the process: $t_w(r,l)$, $t_{wi}(r,l)$, $t_{wo}(r,l)$, $t_{ci}(r,l)$, $t_m(r)$;
- inert gas concentration in the thermal layers of successive rows of tubes: $c_g(r)$;
- partial air and steam pressures in the steam-gas sublayer of a thermal layer: $p_{vci}(r,l)$, $p_{vm}(r,l)$, $p_{gci}(r,l)$, $p_{gm}(r,l)$;
- overall heat transfer coefficient $h(r,l)$ with local convective components: $h_{cw}(r,l)$, $h_{cc}(r,l)$, $h_{cm}(r,l)$;
- heat fluxes per unit area $\Delta q(r,l)$.

The calculation results are comparable with the data obtained from the experimental investigations [1,2,40,41] and calculations [5,6,28,29]. The essential data needed in assessing the irreversible heat transfer include distributions of thermodynamic parameters on the boundaries of thermal layers. The calculations were performed as follows: for the surface of the entire condenser (i.e., both condenser passes), for successive bundles in both passes, and for successive tube rows in each bundle. In total, the calculations were performed for 32 tube rows (23 rows in pass 1 and 9 rows in pass 2). The results of the calculations can be presented in two directions, i.e., along the length of selected tube, l, and across thermal boundaries surrounding the analysed heat transfer surface. The analysis results (presented below) refer only to a selected number of cases. The two extreme cases are the most important. One refers to the heat transfer surfaces on which most intensive condensation processes take place. These surfaces represent the first rows of tubes in the condensation bundles of the first pass (pass 1, $r = 1$). The other refers to the surfaces where the process has the largest air concentration. These surfaces, in turn, are the last rows of tubes in the first condenser pass, i.e., the last rows of air concentration bundles (pass 1, $r = 23$). The results of calculations for the remaining tube rows in the condenser and their interpretations fall between the above extreme cases. On the basis of these results, one can determine where air concentration is the highest, i.e., places from which harmful gases should be sucked out.

6.1 Temperature distributions on thermal boundary layers of fluids involved in the condensation process along the tubes

The most interesting calculation results deserving further detailed analysis concern temperature distributions on the thermal boundary layers of all the fluids involved in the steam condensation process. In total, in accordance with the classification of the heat transfer surfaces, 32 tube rows of the two passes were calculated. Of these, only the two extreme cases are presented. Both cases concern first pass tubes in the first row of condensation bands (pass 1, $r = 1$) and the last row of air concentration bundles (pass 1, $r = 23$).

Selected as characteristic examples, presented below are the temperature distributions on the thermal boundary layers of fluids as functions of tube length, l, in the first row of first pass condensation bundles (pass 1, $r = 1$). Undoubtedly, this is the condenser surface where condensation is most intensive.
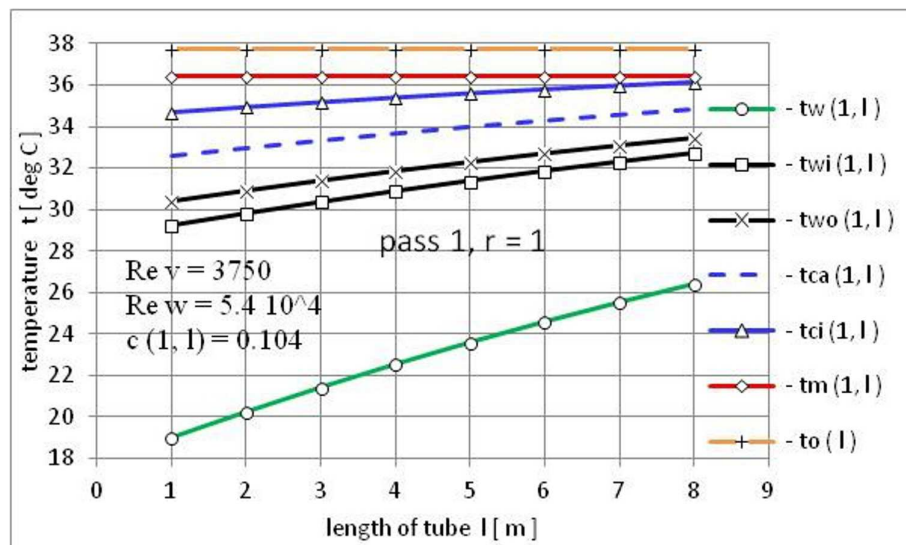

Figure 4: Temperature distributions in the thermal layers of fluids contributing to steam condensation along the first coolant pass tubes pass and in the first condensation bundle row $r = 1$.

The temperature change curves of the thermal layers of fluids around first pass, first row tubes are shown in Fig. 4 as functions of the tube length.

These curves are typical of temperature distributions in all other fluid thermal layers along the tubes. In all remaining cases the only changing parameter is the temperature difference in the cross sections of particular layers. For the analysed tube row (pass 1, $r = 1$), local temperature differences can be ordered as follows:

$$\left[t_{wi}(r,1) - t_w(r,1)\right] > \left[t_{ci}(r,l) - t_{wo}(r,l)\right] > \left[t_0 - t_{ci}(r,l)\right] > \left[t_{wo}(r,l) - t_{wi}(r,l)\right]$$

with $r = 1$ and an arbitrary coordinate l for the interval $1 < l < L$. The highest local temperature difference in the thermal layer of a fluid was recorded in the cooling water. The maximal, dominating value of this difference in the entire calculation process, was recorded in the cooling water inlet section for (pass 1, $r = 1$, $l = 1$) and equalled $[t_{wi}(1,1) - t_w(1,1)]_{max} = 10.26$ K. The second highest local temperature difference was in the condensate layer. The maximal value of condensate temperature difference in the entire calculation process was recorded in the cooling water inlet section for (pass 1, $r = 1$, $l = 1$) and equalled $[t_{ci}(1,1) - t_{wo}(1,1)]_{max} = 4.31$ K. The third highest local temperature difference of the thermal layers in Fig. 4 was in the steam-air mixture layer. Its maximal value was recorded for ($r = 1$, $l = 1$) and equal to $[t_0 - t_{ci}(1,1)]_{max} = 2.38$ K. The lowest local temperature difference in the analysed case (Fig. 4), was on the fouled walls tubes. This was recorded in the cooling water outlet section ($r = 1$, $l = 8$) and equalled $[t_{wo}(1,8) - t_{wi}(1,8)]_{max} = 0.8$ K.

Temperature differences in the cross-sections of all analysed layers decreased along the tube length. The average temperature of the steam-air mixture $t_m(r,l) = t_m(r)$ was constant in all analysed cases, as a consequence of the adopted assumption that air concentration along tubes in successive rows is constant. The average temperature, $t_{ca}(r,l)$, in the condensate layer increased with the increasing temperature, $t_w(r,l)$, of the cooling water, which could be observed by measuring the temperature at the bottom of the working condenser.

The second extreme case concerns air concentration bundles situated at the end of the steam-air mixture flow path in the condenser (pass 1, $r = 23$). According to Fig. 2, the temperature increase of the cooling water heated in the last tube rows is equal to as little as $t_w(23,8) - t_w(23,1) = 1.57$ K. This value and the constant temperature of the steam-air mixture allowed for the calculation of the temperature in thermal layers surrounding the last bundle tubes. The obtained results are shown in Fig. 5.

The order of local temperature differences in the above temperature
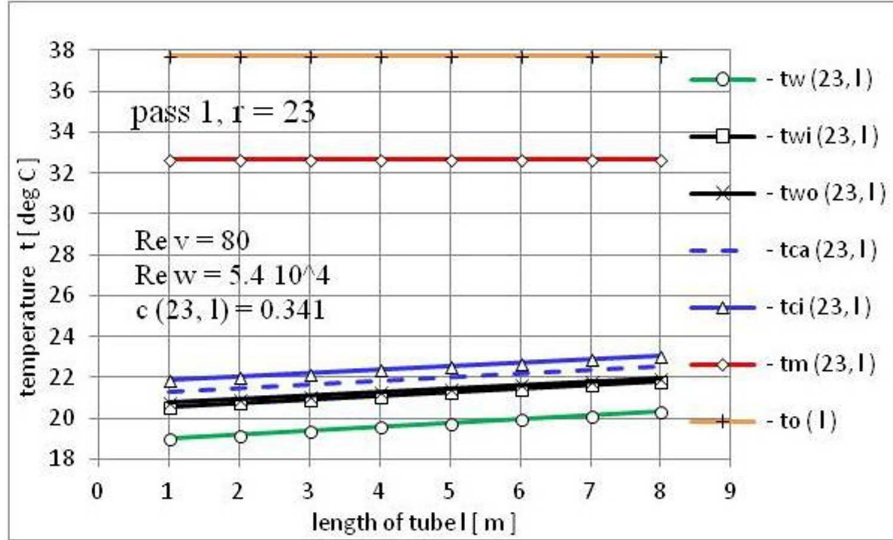
Figure 5: Temperature distributions in thermal layers of fluids contributing to steam condensation along the tubes in the last row $r = 23$ of the air concentration (air cooler) bank.

distributions is as follows:

$$[t_0 - t_{ci}(r, l)] > [t_{wi}(r, 1) - t_w(r, 1)] > [t_{ci}(r, l) - t_{wo}(r, l)] > [t_{wo}(r, l) - t_{wi}(r, l)]$$

with $r = 23$ and arbitrary coordinate l for the interval $1 < l < L$.

Here the highest temperature difference is recorded in cross-sections of the steam-air mixture layers. The maximal value of this difference in the entire calculation was recorded in the cooling water inlet section ($r = 23$, $l = 1$) and was equal to $[t_0 - t_{ci}(23, 1)]_{max} = 15.84$ K. These heat exchange surfaces are in contact with the coldest condensate. The difference between the average temperature of the condensate on the tube and the saturation temperature for the condenser pressure $[t_0 - t_{ca}(23, 1)]_{max}$ is defined as the highest 'condensate super-cooling in the condenser' [8,9,24]. The maximal value of the Jakob number for the condensate flowing around the last tube rows in the air concentration bundles meets condition 6, Subsec. 4.2: Ja $< 2.6 \times 10^{-2}$. The performed calculations show that the lowest temperature in the thermal layers of the steam-air mixture, $t_m(23, l) = t_m(23)$, is observed around the last row tubes of the air cooler bundles. At the same time it is the place where the condensate temperature, $t_{ca}(23, 1)$, is the lowest. That is why this part of the condenser is

called the 'cold end'. Constant pressure of the steam-air mixture in the entire condenser space is the reason why here the highest air concentrations in the mixture are to be expected (according to designers' intentions).

The lowest local temperature difference in the analysed case was on the surfaces of fouled walls tubes. The lowest value of this difference in the entire calculation was recorded in the fouled walls cross section for (pass 1, $r = 23$, $l = 8$) and it was equal to $[t_{wo}(23,8) - t_{wi}(23,8)]_{min} = 0.2$ K.

6.2   Entropy increase in thermal layers of the fluids and in the exchanger diaphragm

It results from the theoretical considerations that the analysis can be based on the data concerning heat transfer between flows of particular fluids [4]. After complementing this data by the information about processes taking place in thermal layers, the analysis of irreversible phenomena can be extended to include these processes, and thus become more precise. Generally, the data for a detailed analysis can be obtained from calculations and/or measurements. Such a detailed analysis is of high importance, as processes taking place in thermal sublayers have a huge impact on the course and results of the entire irreversible phenomenon.

The calculated entropy increases taking place in the process of heat transfer through successive thermal sublayers around the extreme heat exchange surfaces in the first pass condensation bundles (pass 1, $r = 1$) and (pass 1, $r = 9$) are shown in Figs. 6 and 7. For the tubes composing the first rows of the first pass condensation bundles (pass 1, $r = 1$) of the analysed condenser, Fig. 6, the highest thermal degradation in the condensation process takes place in the thermal layers of cooling water, then in the condensate film [21], the sublayer containing NCGs, and finally in the tube walls. In successive rows of tubes composing the first pass condensation bundles the irreversible processes are subject to re-evaluation. Due to the increased NCGs concentration around the heat exchange surfaces (as a result of the decreased Reynolds number), the entropy increase connected with the irreversible heat flow in the layer of steam-gas mixture becomes bigger, Fig. 7. However, the dominating effect is still the entropy increase in the cooling water thermal layers [21,28,29]. The number of tubes in the first pass condensation bundles is the highest.

The next two diagrams, Figs. 8 and 9 present local entropy increases in thermal layers surrounding extreme tube rows in the air concentration (air cooler) bundles.
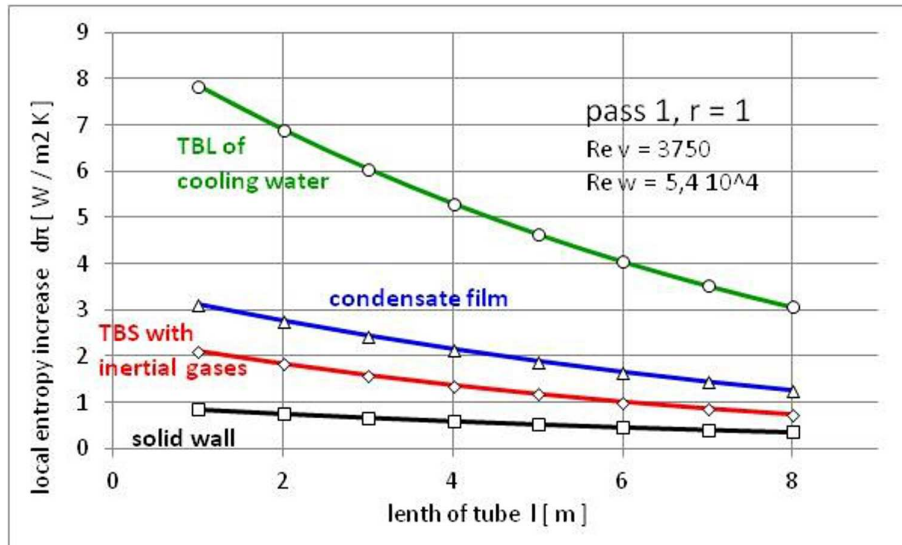
Figure 6: Local entropy increases caused by heat transfer in thermal boundary layers and tube walls of the first row $r = 1$, of the first pass condensation bundles.
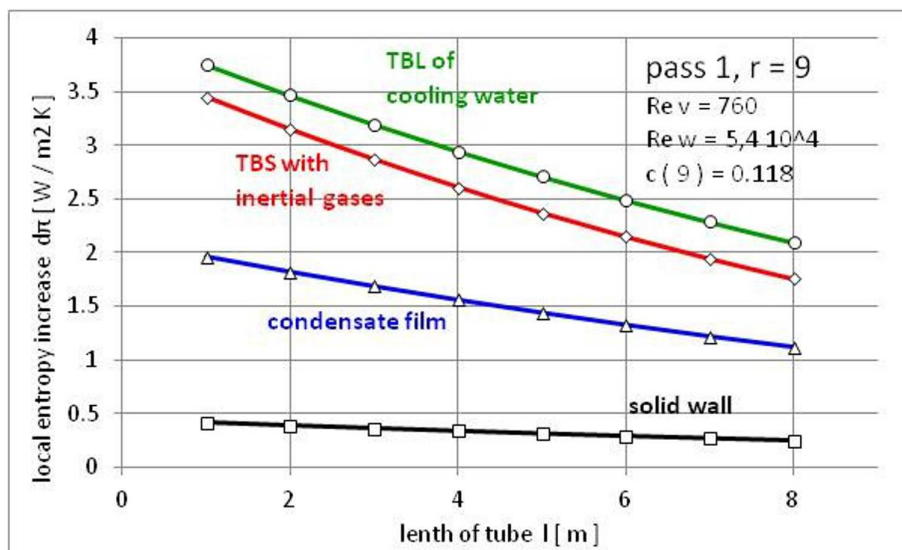

Figure 7: Local entropy increases caused by heat transfer in thermal boundary layers and tube walls of the last row $r = 9$, of the first pass condensation bundles.
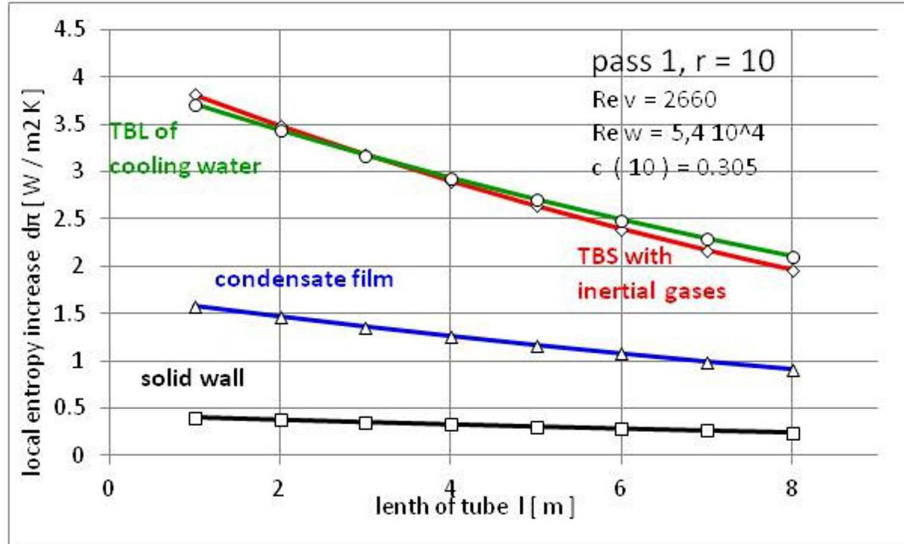
Figure 8: Local entropy increases caused by heat transfer in thermal boundary layers and tube walls of the first row, $r = 10$, of the air concentration bundles.

When the steam-air mixture flows between successive rows of tubes, the proportion of thermal degradation in the steam-gas sublayer increases to reach the same level as that in the thermal layers of cooling water Fig. 8. In the air concentration bundles $10 \leq r \leq 23$ it is the steam-gas sublayer which is decisive for the energy degradation process, with lower contributions represented by, consecutively, the cooling water layer, condensate film, and finally the heat flow through tube walls [21,42], as is illustrated in Figs. 8 and 9. As NCGs concentration increases, heat transfer decreases which, consequently, reduces the entropy increase [28,29]. The results of the performed calculations reveal that the air concentration bundles plays its role well, but at the expense of involving 22% of water flowing through the first pass of the condenser.

The last diagram in these series, selected as the illustration of the calculated results, presents the local entropy increase along last row tubes in the second pass of the condenser (pass 2, $r = 9$). The presented sample case, Fig. 10, of heat exchange surface in last tube rows of the second pass with local degradation of entropy increases is characteristic for the second pass condensation bundles (pass 2, $1 \leq r \leq 9$).
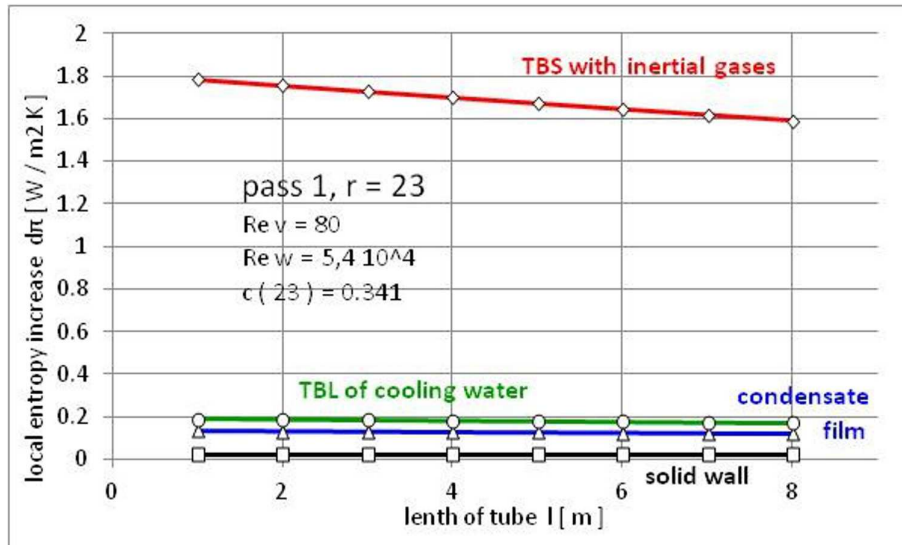
Figure 9: Local entropy increases caused by heat flow in thermal boundary layers and tube walls of the last row, $r = 23$, of the air concentration bundles.
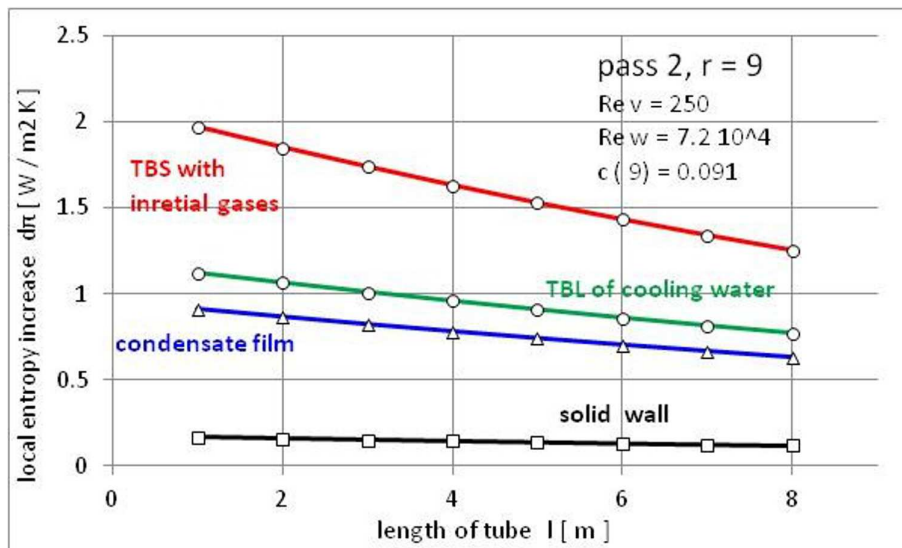

Figure 10: Local entropy increases caused by heat transfer in thermal boundary layers and tube walls of the last row, $r = 9$, of the second pass condensation bundles.

The local entropy increase in the analysed thermal layers is a function of local temperature differences on their boundaries. The higher the temperature difference in the layer, the higher the local entropy increase [28,29]. As further consequences, the local thermal resistance also increases, while the local convective heat transfer coefficient in the layer decreases. Some information on heat flow processes in thermal layers can be gained from analysing the calculated local values of the two latter parameters [20,21]. However, this analysis will not provide opportunity to evaluate the measure of irreversibility of the phenomena taking place in the layers. This opportunity is provided by calculating the entropy increase in the heat flow process.

The last diagrams show the potential of accurate analysis of irreversible heat flow processes in individual (sub)layers and in the partition wall. By summing up local entropy increases in thermal layers around the tubes we can calculate the entropy increases relating to the heat flow between the fluids. A sample analysis of this type is shown in the diagram in Fig. 11.
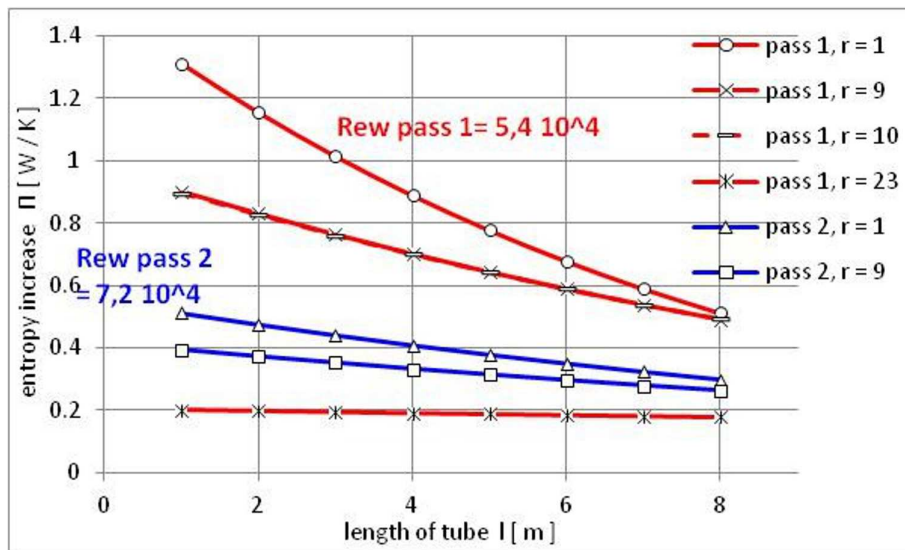

Figure 11: Entropy increases caused by heat transfer in thermal layers and tube walls along the tubes of the first and second passes.

Entropy increases in successive layers can be summed up to assess the thermal degradation of the entire heat transfer process. The results are shown in Fig. 11 for the first and second condenser passes, respectively.

The integral, over the entire surface, of entropy, Π, increases caused by irreversible heat flow in the condenser [4] loaded with a very large air flow (TTD = 9.5 K) is equal to $\Pi = 51.67$ kW/K. It is distributed into particular surfaces as follows:

first pass condensation bundles: $\quad \Pi_{(\text{pass } 1, 1 \leq r \leq 9)} = 31.98$ kW/K$= 0.62\Pi$,

air concentration bundles: $\qquad\quad \Pi_{(\text{pass } 1, 10 \leq r \leq 23)} = 5,40$ kW/K$= 0.11\Pi$,

second pass condensation bundles: $\quad \Pi_{(\text{pass } 2, 1 \leq r \leq 9)} = 14.29$ kW/K$= 0.28\Pi$.

In a correctly operating airtight condenser, TTD = 3.5 K, the total entropy increase over the entire surface is approximately equal to $\Pi = 29.01$ kW/K.

7   Conclusions

The obtained results allow for the recognition of processes which contribute in varying degrees to irreversible energy degradation during steam condensation in various parts of the examined device.

This paper describes a proposal for the analysis of steam condensation in a power plant condenser. The proposed method is illustrated by carrying out a detailed analysis of steam condensation from a mixture with NCGs. This includes calculations based on the Berman model, which takes into account the presence of NCGs in the non-homogeneous process. The phenomenological model of the process is described, necessary assumptions adopted in the method and basic equation describing the phenomenon are presented. Despite a series of adopted simplifying assumptions, the model describes with sufficient precision the phenomenon of steam condensation in a real condenser. A comparison of the calculated results with those from experiments [1–3] allows for the conclusion that they sufficiently well describe real processes taking place on tube surfaces in condenser bundles. The Berman method makes it possible to obtain analytically the distributions of thermodynamic parameters on thermal boundary layers, which are necessary for further precise analyses of irreversible processes. The set of assumptions, making the basis for the presented method, may serve as a starting point for discussion on the development of a more complex model. The device selected for the analysis is well known and tested, though its structure is not optimal.

The analysis has confirmed that the presence of air in the thermal layer significantly disturbs the condensation process. The harmful effect of the

presence of these gases on the process manifests itself by increased pressure in the device, which limits the expansion line in the turbine and thus decreases the efficiency of the entire cycle. While the examined devices have well arranged flow ducts for cooling water and condensing steam, there appears to be a need for the improvement of the arrangement of NCG flows in the steam spaces.

However, the process which is most heavily loaded with entropy increase is heat convection in the cooling water boundary layers. The results of the analysis fully comply with the results of similar analyses based on heat flow resistances, or heat transfer coefficients. Hence, the obtained results and their interpretations make a good basis for further theoretical and applied analyses.

Based on the calculation results, an evaluation of entropy increases caused by heat flow through successive thermal layers made it possible to determine gradation of the irreversibility problem. The highest dominating energy degradation in heat transfer during condensation (additionally filled with air) takes place in the thermal layers of cooling water $\Pi_w = 21.393$ kW/K. The next active layers in the energy degradation process are: thermal layers of the steam-gas sublayer $\Pi_m = 17.176$ kW/K, the layer of the condensate flowing around the vibrating tubes $\Pi_c = 10.491$ kW/K and the irreversible heat flow through the fouled surfaces of the tubes, $\Pi_r = 2.608$ kW/K.

References

[1] Marto P.J., Nunn R.H.: *Power condensers heat transfer technology: Computer Modelling/Design/Fouling.* Hemisphere. Washington, New York, London 1980.

[2] Szklowier G.G., Milman O.O.: *Experimental tests and numerical calculations of steam turbine condensing systems.* Eniergoatomizdat, Moscow 1985 (in Russian).

[3] Chmielniak T.: *Power engineering technology.* WPŚ, Gliwice 2004 (in Polish).

[4] Drozynski Z.: *Entropy increase as a measure of energy degradation in heat transfer.* Arch. Thermodyn. **34**(2013), 3, 147–160.

[5] Butrymowicz D., Trela M.: *Effects of fouling and inert gases on performance of recuperative feedwater heaters.* Arch. Thermodyn. **23**(2001), 1-2, 127–140.

[6] Butrymowicz D., Trela M.: *Problems of condensation heat transfer in power plant heat exchangers.* Trans. Inst. Fluid-Flow Mach. **113**(2003), 107–118.

[7] THIEL G., LIENHARD J.: *Entropy generation in condensation in the presence of high concentrations of noncondensable gases.* Int. J. Heat Mass Tran. **55**(2012), 19-20, 5133–5147.

[8] HUIQIANG XU, ZHONGNING SUN, HAIFENG GU, HAO LI: *Experimental study on the effect of wall-subcooling on condensation heat transfer in the presence of non-condensable gases in a horizontal tube.* Ann. Nucl. Energy **90**(2016), 9–21.

[9] BIN REN, LI ZHANG, HONG XU, ZHENYU TAO: *Experimental study on condensation of steam/air mixture in a horizontal tube.* Exp. Therm. Fluid Sci. **58**(2014), 145–155.

[10] JAFARIAN A., AZIZI M., FORGHANI P.: *Experimental and numerical investigation of transient phenomena in vacuum ejectors.* Energy **102**(2016), 528–536.

[11] COLBURN A., HOUGES O.: *Design of cooler condensers for mixture of vapour with noncondensing gases.* Ind. Eng. Chem. **26**(1934), 11, 1178–1182.

[12] BERMAN L.D., FUKS S.N.: *Mass transfer in condensers with horizontal tubes in the presence of air in the steam.* Tieploeniergetika **5**(1958), 8, 66–74 (in Russian).

[13] BERMAN L.D., FUKS S.N.: *Calculations of surface heat exchangers for steam condensation from steam-air mixture.* Teploenergetika **7**(1959), 6, 74–84 (in Russian).

[14] BERMAN C.C.: *Calculations of turbine heat exchangers.* National Energy Publishers, Moscow 1962 (in Russian).

[15] BERMAN L.D., TUMANOV V.A.: *Investigation of heat transfer during the condensation of flowing steam on horizontal tube bundle.* Teploenergetika **10**(1962), 9, 77–83, (in Russian).

[16] BERMAN L.D.: *Approximation method of heat transfer in steam condensation calculations on horizontal tube bundle.* Teploenergetika **12**(1964), 3,74–78 (in Russian).

[17] BERMAN L.D.: *Heat transfer in steam condensation in around horizontal tube flow, convective heat transfer in one and multiphase flow.* Energia (1964), 7–53 (in Russian).

[18] BERMAN L.D.: *Determining the mass transfer coefficient in calculations on condensation of steam containing air.* Teploenergetika **16**(1968), 66–71 (in Russian).

[19] BERMAN L.D.: *Influence of velocity on heat transfer in steam condensation around horizontal tube.* Teploenergetika **5**(1979), 16–20 (in Russian).

[20] RUSOWICZ A.: *Numeric simulation of condenser power plant 50 MW.* Arch. Energ., XXXVI(2006).

[21] GRZEBIELEC A., RUSOWICZ A.: *Thermal resistance of steam condensation in horizontal tube bundles.* J. Power Technologies **91**(2011), 1, 41–48.

[22] TRELA M., BUTRYMOWICZ J. ET AL.: *Monitoring of air content in a mixture removed from condensers in application to steam turbine diagnostics.* In: Proc. Int. Joint Power Generation Conf. Miami Beach 2000.

[23] DROZYNSKI Z.: *Phenomenological model of steam condensation containing noncondensable gases on a single non-inundated tube.* Arch. Thermodyn. **27**(2006), 4, 67–78.

[24] STRUŠNIK D., GOLOB M., AVSEC J.: *Effect of non-condensable gas on heat transfer in steam turbine condenser and modelling of ejector pump system by controlling the gas extraction rate through extraction tubes.* Energ. Convers. Manage. **126**(2016), 228–246.

[25] NUSSELT W.: *Die oberflachenkondensation des wasserdampfes.*, Vereins Deutcher Ing., 1916.

[26] WISNIEWSKI S, WISNIEWSKI T.: *Heat Transfer.* WNT, Warszawa 2000.

[27] BRIGGS A., SABARATNAM S.: *Condensation from pure steam-air mixtures on integral fin tubs in a bank.* J. Heat Transfer **127**(2005), 6, 571–580.

[28] HASELI Y., DINCER I., NATERER G.F.: *Entropy generation of vapour condensation in the presence of a non condensable gas in a shell and tube condenser.* Int. J. Heat Mass Tran. **51**(2008), 7–8, 1596–1602.

[29] HASELI Y., NATERER G.F., DINCER I.: *Thermal effectiveness of a shell and tube condenser with effects of non-condensing gas leakage.* In: Proc. 40th AIAA Thermophysics Conf., Seattle, June 23-26, 2008.

[30] CLAUSIUS R.: *Ueber die bewegende Kraft der Waerme und die Gesetze, welche sich daraus fuer die Waermelehre selbst ableiten lassen.* Pogendorff Annalen, Tyndall j., Phil. Mag. 1851.

[31] BEJAN A.: *Advanced Engineering Thermodynamics.* J. Wiley & Sons, New York 1988.

[32] BEJAN A.: *Entropy generation minimization, exergy analysis, and the constructal law arab.* J. Sci. Eng. **38**(2013), 329–340.

[33] HASELI Y., DINCER I., NATERER G.: *Entropy generation of vapour condensation in the presence of a non-condensable gas in a shell and tube condenser.* Int. J. Heat Mass Tran. **51**(2007), 7–8, 1596–1602.

[34] GALOVIC A., VIRAG Z., ZIVIC M.: *Analytical entropy analysis of recuperative heat exchanger.* Entropy **5**(2003), 482–495.

[35] OCHEDUSZKO S.: *Applied Thermodynamics.* WNT, Warszawa 1970.

[36] KLEIN S., NELLIS G.: *Thermodynamics.* Cambridge University Press, 2012.

[37] BORGNAKE C., SONNTAG R.: *Fundamentals of Thermodynamics.* Wiley, 2013.

[38] WENTERODT T., REDECKER C., HERWIG H.: *Second law analysis for sustainable heat and energy transfer: The entropic potentials concept.* Appl. Energy **139**(2015), 376–383.

[39] NARAYAN G.P., LIENHARD J.H., ZABIR S.M.: *Entropy generation minimization of combined heat and mass transfer devices.* Int. J. Therm. Sci. **49**(2010), 10, 2057–2066.

[40] BRIGGS A., SABARATNAM S.: *Condensation of steam in the presence of air on a single tube and a tube bank.* Int. J. Energ. Res. **27**(2003), 4, 301–314.

[41] BRIGGS A., SABARATNAM S.: *Condensation from pure steam-air mixtures on integral –fin tubs in a bank.* J. Heat Transfer **127**(2004), 6, 571–580.

[42] RUSOWICZ A., LASKOWSKI R., GRZEBIELEC A.: *The numerical and experimental study of two passes power plant condenser.* Therm. Sci. **21**(2017), 1A, 353–362.